Catalytic performance of indium-supported TiO_2–ZrO_2 for the selective reduction of nitrogen monoxide in the presence of oxygen

Yoshiaki Kintaichi, Masaaki Haneda *, Megumu Inaba and Hideaki Hamada

National Institute of Materials and Chemical Research, Higashi, Tsukuba, Ibaraki 305, Japan
E-mail: hane@nimc.go.jp

Received 4 April 1997; accepted 14 July 1997

The catalytic activity of indium-supported TiO_2–ZrO_2 binary metal oxide for the selective reduction of NO with propene in the presence of oxygen was investigated. The supported indium caused a drastic enhancement of NO reduction activity of TiO_2–ZrO_2. It was suggested that the "dispersed phase" of indium oxide, which is reduced at lower temperature in temperature-programmed reduction (TPR), is responsible for the high activity. Propene served as the most efficient reducing agent, while oxygenated hydrocarbons were not good ones. A reaction mechanism was proposed that N_2 is formed through the reaction of propene and NO_2, which was formed on the acid sites of TiO_2–ZrO_2, on the indium sites.

Keywords: nitrogen monoxide, selective reduction, binary oxide, In-supported TiO_2–ZrO_2, TPR

1. Introduction

The selective catalytic reduction of nitrogen oxides (NOx) with hydrocarbons in the presence of excess oxygen is attracting much attention from a viewpoint of practical applications to the deNOx system of diesel and lean-burn gasoline engine exhausts [1]. Many catalysts for this reaction have been reported after Cu ion-exchanged ZSM-5 catalyst was discovered by Held et al. [2] and Iwamoto et al. [3], following patent literature [4,5]. Although most of them were related to zeolite-based catalysts such as Ce- [6], Pt- [7], H-ZSM-5 [8], Co-beta [9] and so on, our group found that single metal oxides such as Al_2O_3 [10] and transition metal-supported alumina [11] also catalyze this reaction. Furthermore, we reported that several binary oxides showed higher activity than their corresponding single metal oxides for NO reduction by propane [12].

Hosose et al. [13] reported that the addition of copper to SiO_2–Al_2O_3 binary oxide enhanced the catalytic activity for NO reduction by ethene. There are, however, few reports concerning the effect of metal additives on the activity of binary oxides. Recently, we reported that silver-supported TiO_2–ZrO_2 catalysts showed high activity for NO reduction by propene in the presence of oxygen and confirmed that TiO_2–ZrO_2 binary oxide can be used as a good catalytic support for this reaction [14].

In many cases the transition metals are loaded on metal oxide supports as an active component to improve the NO reduction activity. Miyadera and Yoshida [15] reported, however, that indium, which is not a transition metal, supported on alumina showed a high catalytic activity for NO reduction by propene. Kikuchi and Yogo [16] also reported that addition of gallium and indium, which are group IIIA metals, to H-ZSM-5 caused an enhancement of the catalytic activity for NO reduction by methane. Hence, some base metals in addition to transition metals also seem to be effective additives toward the title reaction.

In the present work, we investigated the additive effect of indium on the activity of TiO_2–ZrO_2 binary oxide for the selective reduction of NO with propene in the presence of excess oxygen. Here, we selected TiO_2–ZrO_2 as the support because of its high BET surface area, which enables preparation of highly dispersed metal supported catalysts. The presence of solid acid or base property on TiO_2–ZrO_2 and the higher heat resistance compared to TiO_2 and ZrO_2 are other reasons for its selection.

In the course of our study, we found that indium enhances the NO reduction activity of TiO_2–ZrO_2 more than silver reported previously [14]. Accordingly, we report here the detailed experimental results on the role of indium for this reaction and would like to discuss a possible reaction mechanism. The efficiency of various hydrocarbons as a reducing agent was also examined.

2. Experimental

2.1. Catalyst preparation

TiO_2–ZrO_2 binary oxide with a molar ratio of unity was prepared according to our previous paper [14]. In brief, the binary oxide was obtained by hydrolyzing a solution containing titanium(IV) tetraisopropoxide and zirconium(IV) tetrapropoxide in 2-propanol, followed by drying at 110°C and calcination at 500°C for 5 h in air

---

* To whom correspondence should be addressed.

stream. Indium-supported catalysts were prepared by immersing TiO_2–ZrO_2 powder in an aqueous solution of $In(NO_3)_3{\cdot}2H_2O$, followed by drying and calcination at 500°C for 5 h in flowing air. Indium loading was changed from 2 wt% to 15 wt% as In metal.

2.2. Catalytic activity measurements

The catalytic activity was measured with a fixed-bed flow reactor by passing a reactant gas containing 900 ppm NO, 10% O_2, a reducing agent and helium as the balance gas at a rate of 66 $cm^3\ min^{-1}$ over 0.2 g of catalyst. CH_4, C_2H_4, C_3H_8, C_3H_6, CH_3OH, C_2H_5OH, 1-C_3H_7OH, 2-C_3H_7OH and $(CH_3)_2CO$ were used as the reducing agent. In order to investigate a reaction pathway, NO_2 (930 ppm) reduction and propene (860 ppm) oxidation by O_2 (10%) were also carried out. The analysis of the effluent gas was made by gas chromatographs equipped with a Molecular Sieve 5A column (for the analysis of N_2, CO and CH_4) and a Porapak Q column (for that of CO_2, N_2O, C_2H_4, C_3H_6 and C_3H_8). The reaction temperature was changed with a step of 50°C from 500 to 200°C.

2.3. Catalyst characterization

BET surface area was measured with a conventional flow apparatus (Shimadzu, Flowsorb II 2300) by nitrogen adsorption at −196°C. The crystal structure was identified by XRD (Shimadzu XD-1) measurements using Cu Kα radiation at 40 kV and 40 mA.

TPR (temperature-programmed reduction) measurements were carried out to estimate the reduction behavior of the indium-supported catalysts. Before the TPR measurement, 0.05 g of the catalyst was placed in a quartz tube reactor and oxidized at 500°C for 1 h in flowing air. 10 vol% H_2–Ar gas mixture was used as a reducing gas with a flow rate of 30 ml min^{-1} and the temperature of the catalyst bed was raised at a heating rate of 5°C min^{-1}. After the outlet gas from the catalyst bed was passed through a silica gel column to eliminate H_2O produced by the TPR operation, the difference in the H_2 concentration between at the inlet and at the outlet of the reactor was detected by a thermal conductivity detector.

3. Results and discussion

3.1. NO reduction activity of indium-supported TiO_2–ZrO_2

Figure 1 shows the catalytic activity of indium-supported TiO_2–ZrO_2 for NO reduction by propene in the presence of 10% oxygen. It is clear that NO conversion to N_2 on TiO_2–ZrO_2 was enhanced drastically from 25 to 60% at 400°C by addition of 2 wt% of indium. Indium loading of more than 5 wt%, however, did not cause a further enhancement of the maximum NO conversion, although the temperature giving the maximum NO conversion shifted to a lower temperature region. The propene oxidation activity increased with indium loading up to 10 wt%, although propene conversion to COx on 15 wt% In/TiO_2–ZrO_2 was almost the same as that on 10 wt% In/TiO_2–ZrO_2.

The ratio of NO conversion to propene conversion can be regarded as the selectivity of this reaction. We calculated the selectivity for NO reduction, defined as the following equation:

$$\text{selectivity} = \frac{\text{number of NO molecules reduced to } N_2}{\text{number of } C_3H_6 \text{ molecules oxidized to COx}}\,.$$

In table 1 are summarized the selectivities on In/TiO_2–ZrO_2 at 350 and 400°C along with the conversions of NO to N_2 and those of propene to COx. The selectivity on

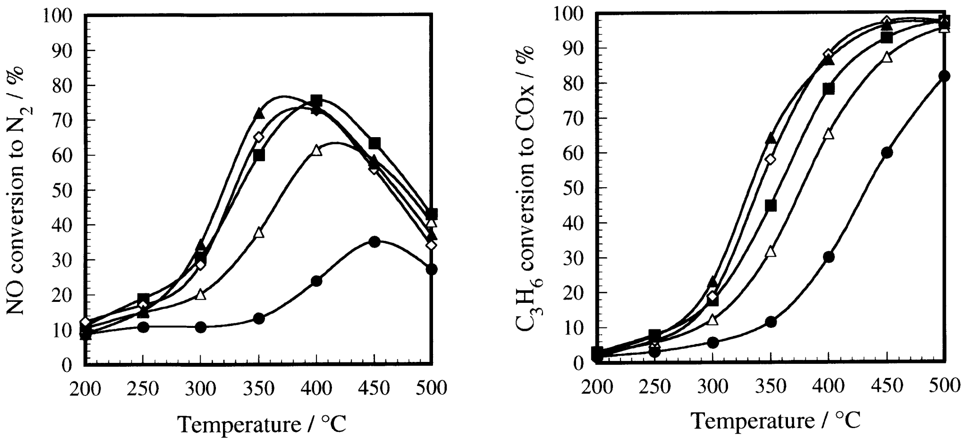

Figure 1. Additive effect of indium in the catalytic activity of TiO_2–ZrO_2 for the selective reduction of NO with propene. Conditions: NO = 900 ppm, C_3H_6 = 860 ppm, O_2 = 10%, catalyst weight = 0.2 g, gas flow rate = 66 $cm^3\ min^{-1}$. (●) TiO_2–ZrO_2, (△) 2 wt% In/TiO_2–ZrO_2, (■) 5 wt% In/TiO_2–ZrO_2, (◇) 10 wt% In/TiO_2–ZrO_2, (▲) 15 wt% In/TiO_2–ZrO_2.

Table 1
Conversions and selectivity over In/TiO_2–ZrO_2 [a]

Catalyst	Reaction temperature (°C)	NO conversion to N_2 (%)	C_3H_6 conversion to COx (%)	Selectivity
TiO_2–ZrO_2	350	13.2	11.5	1.22
	400	23.8	30.0	0.85
2% In/TiO_2–ZrO_2	350	37.9	31.7	1.32
	400	61.3	65.4	1.00
5% In/TiO_2–ZrO_2	350	60.0	44.8	1.46
	400	75.4	78.1	1.03
10% In/TiO_2–ZrO_2	350	65.0	57.9	1.24
	400	72.7	87.9	0.89
15% In/TiO_2–ZrO_2	350	72.1	64.2	1.20
	400	73.4	86.5	0.89

[a] Conditions: NO = 900 ppm, C_3H_6 = 860 ppm, O_2 = 10%, catalyst weight = 0.2 g, gas flow rate = 66 $cm^3\ min^{-1}$.

In/TiO_2–ZrO_2 increased gradually with indium loading and reached a maximum at about 5 wt%. This means that indium loaded on TiO_2–ZrO_2 accelerates the reduction of nitrogen oxides by propene. However, in the region above 10 wt% of indium loading, the selectivity turned to a decrease. This would be ascribed to the promotion of the direct oxidation of propene by oxygen, which decreases the selectivity, by excess amounts of indium.

3.2. Morphology of indium species supported on TiO_2–ZrO_2

BET surface area of In/TiO_2–ZrO_2 catalysts was measured together with that of the support. The results are summarized in table 2. The BET surface area of TiO_2–ZrO_2 was about 280 $m^2\ g^{-1}$, but it decreased monotonously with increasing indium loading. This can be attributed to a blockage of the pores of TiO_2–ZrO_2 by supported indium. In order to examine the crystallite structure of the supported indium, XRD measurements were carried out. As can be seen in figure 2, no diffraction peaks assigned to indium compounds were observed in the XRD patterns of all the In/TiO_2–ZrO_2 catalysts. Indium seems to be highly dispersed on TiO_2–ZrO_2 support.

Figure 3 shows the result of TPR measurements carried out to clarify the morphology of indium on TiO_2–ZrO_2. Two reduction peaks in the temperature regions between 200 and 300°C and above 500°C were observed in the TPR profiles of indium-supported TiO_2–ZrO_2 catalysts. These peaks are attributed to the reduction of supported indium oxide, because no outstanding reduction peaks were detected in the TPR profile of TiO_2–ZrO_2 itself below 500°C. It is considered that indium oxide supported on TiO_2–ZrO_2 consists of two species: one is a dispersed phase species reducible at low temperature and the other is a bulk phase species reducible at high temperature. On the other hand, pure In_2O_3 as a standard sample did not show clear reduction peaks, but was reduced slowly in the temperature region above 500°C. This is probably because In_2O_3 is made up of only large particles of the "bulk phase", suggested by its low BET surface area (74 $m^2\ g^{-1}$).

Apparently, the temperature of both reduction peaks shifted to low temperature region with indium loading up to 10 wt%, and the reduction behavior of In species on 15 wt% In/TiO_2–ZrO_2 was almost the same as that on 10 wt% In/TiO_2–ZrO_2. This fact suggests that the indium dispersion does not change more than 10 wt% indium loading. The relative peak areas of the peak around

Table 2
BET surface areas and relative peak areas of the peak around 250°C in TPR profiles of In/TiO_2–ZrO_2

Catalyst	BET surface area ($m^2\ g^{-1}$)	TPR profiles	
		temperature of peak below 500°C (°C)	relative area of the peak around 250°C [b]
TiO_2–ZrO_2	284	n.d. [a]	–
2% In/TiO_2–ZrO_2	212	275	100
5% In/TiO_2–ZrO_2	206	250	176
10% In/TiO_2–ZrO_2	184	230	201
15% In/TiO_2–ZrO_2	162	230	198
In_2O_3	74	n.d. [a]	–

[a] n.d. means that the peak was not detected in the temperature region below 500°C.

[b] Normalized based on the peak area of 2% In/TiO_2–ZrO_2.

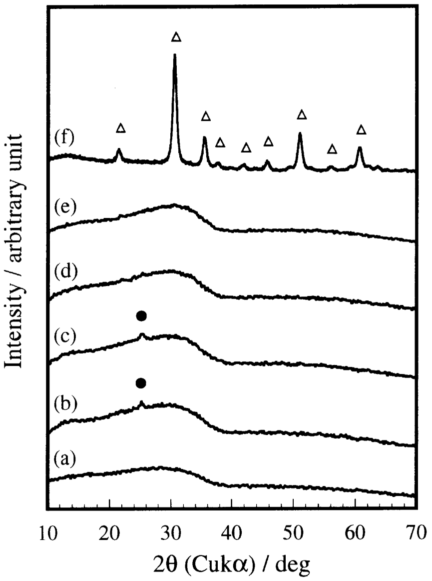

Figure 2. X-ray diffraction patterns of (a)TiO_2–ZrO_2, (b) 2 wt% In/ TiO_2–ZrO_2, (c) 5 wt% In/TiO_2–ZrO_2, (d) 10 wt% In/TiO_2–ZrO_2, (e) 15 wt% In/TiO_2–ZrO_2 and (f) pure In_2O_3 as standard. (●) TiO_2 (anatase), (△) In_2O_3.

250°C, normalized based on the peak area of 2 wt% In/ TiO_2–ZrO_2, were also summarized in table 2. It is noteworthy that the relative peak area increased gradually up to 10 wt% of In loading. This tendency is consistent with that of NO reduction activity. On the basis of these results, we concluded that the "dispersed phase" of indium oxide, which is reduced at low temperature, is the active species for NO reduction and is responsible for the activity enhancement.

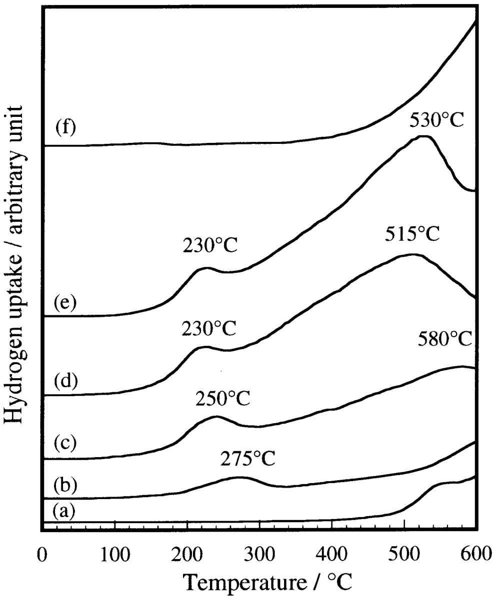

Figure 3. TPR profiles of (a) TiO_2–ZrO_2, (b) 2 wt% In/TiO_2–ZrO_2, (c) 5 wt% In/TiO_2–ZrO_2, (d) 10 wt% In/TiO_2–ZrO_2, (e) 15 wt% In/ TiO_2–ZrO_2 and (f) pure In_2O_3 (standard) after oxidation at 500°C for 1 h. Conditions: catalyst weight = 0.05 g, gas flow rate = 30 cm^3 min^{-1}, heating rate = 10°C min^{-1}, reducing gas: 10% H_2–Ar.

3.3. Efficiency of the reducing agent

The efficiency of various reducing agents for the selective reduction of NO over 5 wt% In/TiO_2–ZrO_2 was investigated. The results are summarized in table 3. For hydrocarbons, methane hardly promoted NO reduction. Ethene and propane were not good reducing agents, either. NO reduction proceeded at relatively high temperatures with these three hydrocarbons. Among hydrocarbons tested here, propene served as the most efficient reducing agent. Oxygenated hydrocarbons did not serve as an efficient reducing agent for NO reduction, compared with hydrocarbons. This would be because they are oxidized by oxygen more easily than their corresponding hydrocarbons. The efficiency increased in the sequence of methanol < ethanol < 1-propanol = acetone < 2-propanol, although exact comparison of the efficiency is impossible because of the different C/NO ratios.

3.4. Reaction mechanism

The reaction pathway of NO reduction by propene over 5 wt% In/TiO_2–ZrO_2 was investigated by measuring the activity for several unit reactions. The reactivity of NO and NO_2 was compared first. Figure 4 presents the reaction results on In/TiO_2–ZrO_2 and on TiO_2–ZrO_2. The reactivity of NO_2 is slightly higher than that of NO at temperatures below 350°C. These facts suggest the participation of NO_2 as an intermediate in NO reduction. It was reported that one of the roles of supported metals is to promote NO oxidation to NO_2, as in the case of Co in Co/Al_2O_3 [17] and Ce in Ce-ZSM-5 [7]. In this work, however, the role of indium on In/TiO_2–ZrO_2 is not to accelerate NO oxidation, because NO_2 conversion to N_2 on TiO_2–ZrO_2 was lower than NO conversion to N_2 on In/TiO_2–ZrO_2. This consideration is also supported by the experimental results for NO oxidation to NO_2 carried out on both TiO_2–ZrO_2 and In/ TiO_2–ZrO_2. The conversion of NO to NO_2 at 400°C was about 28% for both catalysts. Clearly, this means that the supported indium does not catalyze NO oxidation to NO_2.

Since the activation of hydrocarbons by NOx and/or O_2 is considered to be another role of supported indium, we examined next the propene conversion to COx for the reaction system of NO + C_3H_6 + O_2, C_3H_6 + O_2 and NO_2 + C_3H_6 + O_2. The results are shown in figure 5. Apparently, the catalytic activity of In/TiO_2–ZrO_2 for propene oxidation by O_2 was almost the same as that of TiO_2–ZrO_2, suggesting that propene combustion by oxygen occurs predominantly on TiO_2–ZrO_2 and that indium does not promote this step. However, the catalyt-

Table 3
Efficiency of various reducing agents for the selective reduction of NO over 5 wt% In/TiO_2–ZrO_2 [a]

Reductant	NO conversion to N_2 (%) (HC conversion to COx (%))				
	300°C	350°C	400°C	450°C	500°C
CH_4	2.3	2.7	4.0	5.4	6.7
2790 ppm	(0.9)	(1.2)	(2.0)	(5.8)	(13)
C_2H_4	8.4	14	22	30	28
1410 ppm	(3.1)	(5.9)	(12)	(24)	(46)
C_3H_6	31	60	75	63	43
860 ppm	(18)	(45)	(78)	(93)	(97)
C_3H_8	2.1	6.3	14	25	25
890 ppm	(0.6)	(3.2)	(10)	(27)	(50)
CH_3OH	2.3	2.2	2.3	2.2	2.4
510 ppm	(98)	(100)	(100)	(99)	(98)
C_2H_5OH	15	22	21	11	8.4
450 ppm	(55)	(79)	(93)	(94)	(98)
1-C_3H_7OH	19	28	29	17	3.6
550 ppm	(49)	(78)	(98)	(99)	(99)
2-C_3H_7OH	16	32	41	33	19
550 ppm	(26)	(65)	(91)	(99)	(100)
$(CH_3)_2CO$	18	28	32	19	9.2
680 ppm	(51)	(81)	(99)	(100)	(100)

[a] Conditions: NO = 900 ppm, O_2 = 10%, catalyst weight = 0.2 g; gas flow rate = 66 cm^3 min^{-1}.

ic activity of TiO_2–ZrO_2 for propene oxidation was depressed considerably by the presence of NO or NO_2. On the other hand, the propene conversion to COx on In/TiO_2–ZrO_2 is almost the same for all the reaction systems. These results agree with the selectivity increase for NO reduction to N_2 by addition of indium, as described above. On the basis of these results, it is considered that propene is activated by the reaction with NOx (NO or NO_2) mainly on indium.

It is well known that TiO_2–ZrO_2 exhibits high surface acidity by a charge imbalance based on the generation of Ti–O–Zr bonding [18]. Hence, it is considered that acid sites of TiO_2–ZrO_2 play an important role for this reaction. There are some reports that the role of acid sites is

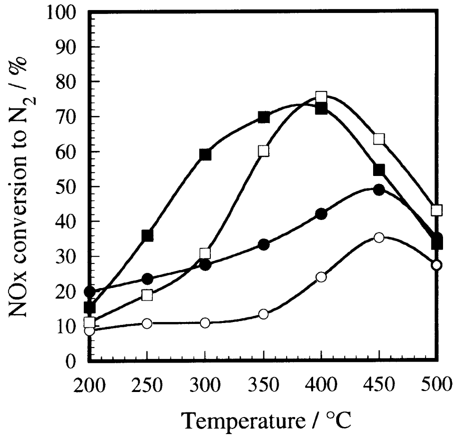

Figure 4. Comparison of reactivity between NO (○, □) and NO_2 (●, ■) for the selective reduction over TiO_2–ZrO_2 (○, ●) and 5 wt% In/TiO_2–ZrO_2 (□, ■). Conditions: NO = 900 ppm or NO_2 = 930 ppm, C_3H_6 = 860 ppm, O_2 = 10%, catalyst weight = 0.2 g, gas flow rate = 66 cm^3 min^{-1}.

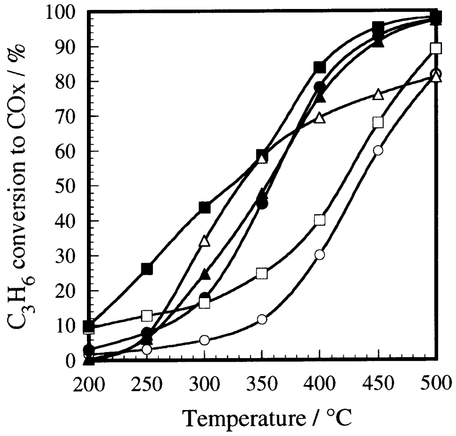

Figure 5. Comparison of the propene conversion to COx for the reaction system of NO + C_3H_6 + O_2 (○, ●), C_3H_6 + O_2 (△, ▲) and NO_2 + C_3H_6 + O_2 (□, ■) over TiO_2–ZrO_2 (○, △, □) and 5 wt% In/TiO_2–ZrO_2 (●, ▲, ■). The reaction conditions are the same as for figure 4.

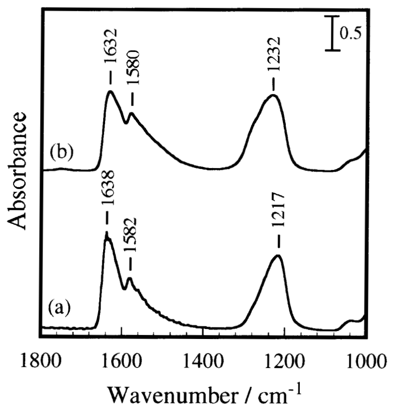

Figure 6. FT-IR spectra of adsorbed species formed on (a) TiO_2–ZrO_2 and (b) 5 wt% In/ TiO_2–ZrO_2 after exposure to a mixture of NO (5 Torr) + O_2 (30 Torr) at room temperature for 30 min, and then evacuation at room temperature for 30 min.

to promote NO oxidation step. For instance, Kikuchi and Yogo reported that acid sites of Ga-ZSM-5, In-ZSM-5 and H-ZSM-5 are responsible for NO oxidation activity, although the detailed mechanism is not clear [16]. In the present study, it is presumed that the acid (or acid–base pair) sites of TiO_2–ZrO_2 catalyze NO oxidation and NO_2 formed thus participates directly in the overall NO reduction. In order to examine surface adsorbed species formed on TiO_2–ZrO_2 and In/ TiO_2–ZrO_2 after exposure to NO + O_2, we carried out in situ IR measurements. FT-IR spectra were recorded in the same manner described elsewhere [19]. A reaction gas composed of NO (5 Torr) and O_2 (30 Torr) was used. As given in figure 6, similar FT-IR spectra were obtained on both TiO_2–ZrO_2 and In/ TiO_2–ZrO_2. All the IR peaks observed here were assigned to NO_3^- species [20]. Since the peak position and the relative peak intensity are almost the same on both catalysts, NO_2-like (NO_3^-) species seems to be formed mainly on TiO_2–ZrO_2.

We also carried out the following experiment concerning the effect of Na additive, which is poisonous material inhibiting the acid sites, to In/ TiO_2–ZrO_2, in order to get detailed information on the role of acid sites of TiO_2–ZrO_2. Na-modified TiO_2–ZrO_2, abbreviated as Na/ TiO_2–ZrO_2, was prepared by immersing TiO_2–ZrO_2 powder in an aqueous solution of Na_2CO_3, followed by drying and calcination at 500°C in flowing air. The content of Na was fixed at 1 wt%. Then, In/Na/ TiO_2–ZrO_2 was prepared by the impregnation method described above in the experimental section. The loading of In was fixed at 5 wt%. BET surface area of this catalyst was found to be 185 $m^2\ g^{-1}$, which is almost the same as that of In/ TiO_2–ZrO_2. We carried out NO–C_3H_6–O_2 and NO_2–C_3H_6–O_2 reactions over In/Na/ TiO_2–ZrO_2. The reaction results as well as those of In/ TiO_2–ZrO_2 are summarized in table 4. Obviously, the addition of Na into In/ TiO_2–ZrO_2 caused a drastic loss of NO reduction activity of In/ TiO_2–ZrO_2 over the whole temperature range, indicating that Na-additive inhibited important steps in this reaction. We think that Na-additive depressed the de-NOx activity of In/ TiO_2–ZrO_2 by weakening the acidity of TiO_2–ZrO_2, because no change in BET surface area of TiO_2–ZrO_2 was observed before and after the addition of Na. If all of the reaction steps take place on the indium sites, NO_2 reduction activity of In/ TiO_2–ZrO_2 and In/Na/ TiO_2–ZrO_2 would be almost the same. However, the former was much higher than the latter. Consequently, we concluded that TiO_2–ZrO_2 plays an important role to form NO_2 and to concentrate NO_2 as NO_3^- on its acid site, and that NO_2 formed thus reacts with propene to form N_2 over In sites. The proposed reaction pathway is illustrated in scheme 1.

4. Conclusions

The catalytic performance of indium-supported TiO_2–ZrO_2 binary metal oxide for the selective reduction of NO with propene was investigated. The supported indium promoted drastically the activity of TiO_2–ZrO_2 for the selective reduction of NO. Optimum indium loading was at 5 wt%. It was suggested that a highly dispersed indium oxide phase is responsible for

Table 4
The influence of Na additive on the catalytic activity of 5 wt% In/ TiO_2–ZrO_2 for NO reduction and NO_2 reduction by propene [a]

Catalyst	Reaction	NOx conversion to N_2 (%) (C_3H_6 conversion to COx (%))				
		300°C	350°C	400°C	450°C	500°C
5% In/ TiO_2–ZrO_2	NO + C_3H_6 + O_2	31 (18)	60 (45)	75 (78)	63 (93)	43 (97)
	NO_2 + C_3H_6 + O_2	59 (44)	70 (59)	72 (84)	54 (95)	33 (98)
5% In/1% Na/ TiO_2–ZrO_2	NO + C_3H_6 + O_2	16 (6.4)	27 (18)	38 (38)	40 (60)	34 (79)
	NO_2 + C_3H_6 + O_2	18 (10)	39 (25)	45 (45)	49 (62)	47 (80)

[a] Conditions: NO = 900 ppm or NO_2 = 930 ppm, C_3H_6 = 860 ppm, O_2 = 10%, catalyst weight = 0.2 g; gas flow rate = 66 $cm^3\ min^{-1}$.

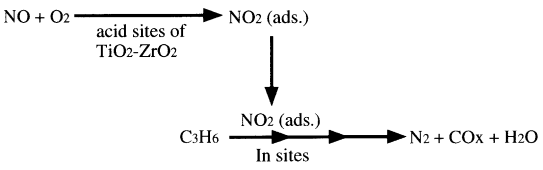

Scheme 1. Proposed reaction pathway of the selective reduction of NO with propene over In/TiO_2–ZrO_2.

the activity enhancement. Although methane, ethane, propane and alcohols were not good reductants, propene served as the most efficient reducing agent. It was found that the acidity of TiO_2–ZrO_2 is essential for NO reduction by propene on In/TiO_2–ZrO_2, by the comparison of that on Na-modified In/TiO_2–ZrO_2. We proposed a reaction pathway on In/TiO_2–ZrO_2 that NO reduction to N_2 proceeds through the reaction of propene and NO_2, which was formed on the acid sites of TiO_2–ZrO_2, on the indium sites.

References

[1] M.D. Amiridis, T. Zhang and R.J. Farrauto, Appl. Catal. B 10 (1996) 203.

[2] W. Held, A. Koenig, T. Richter and L. Puppe, SAE Paper 900496 (1990).

[3] M. Iwamoto, H. Yahiro, Y. Yu-u, S. Shundo and N. Mizuno, Shokubai (Catalyst) 32 (1990) 430.

[4] Ger. Offen. DE 3,642,018 (1987), to Volkswagen A.G.

[5] Ger. Offen. DE 3,735,151 (1988), to Toyota Co.

[6] C. Yokoyama and M. Misono, Catal. Today 22 (1994) 59;
C. Yokoyama and M. Misono, J. Catal. 150 (1994) 9.

[7] M. Iwamoto, H. Yahiro, H.K. Shin, M. Watanabe, J. Guo, M. Konno, T. Chikahisa and T. Murayama, Appl. Catal. B 5 (1994) L1.

[8] H. Hamada, Y. Kintaichi, M. Sasaki, T. Ito and M. Tabata, Appl. Catal. 64 (1990) L1.

[9] T. Tabata, M. Kokitsu, H. Ohtsuka, O. Okada, L.M.F. Sabatino and G. Bellussi, Catal. Today 27 (1996) 91.

[10] Y. Kintaichi, H. Hamada, M. Tabata, M. Sasaki and T. Ito, Catal. Lett. 6 (1990) 239.

[11] H. Hamada, Y. Kintaichi, M. Sasaki, T. Ito, T. Yoshinari, M. Tabata, F. Suganuma and H. Tsuchida, in: *Advanced Materials'93, V/A: Ecomaterials*, Vol. 18A, ed. R. Yamamoto (Elsevier, Amsterdam, 1994) pp. 421–424.

[12] M. Tabata, H. Hamada, Y. Kintaichi, M. Sasaki and T. Ito, Sekiyu Gakkaishi 36 (1993) 191.

[13] H. Hosose, H. Yahiro, N. Mizuno and M. Iwamoto, Chem. Lett. (1991) 1859.

[14] M. Haneda, Y. Kintaichi, M. Inaba and H. Hamada, Bull. Chem. Soc. Jpn. 70 (1997) 499.

[15] T. Miyadera and K. Yoshida, Chem. Lett. (1993) 1483.

[16] E. Kikuchi and K. Yogo, Catal. Today 22 (1994) 73.

[17] H. Hamada, Y. Kintaichi, M. Inaba, M. Tabata, T. Yoshinari and H. Tsuchida, Catal. Today 29 (1996) 53.

[18] K. Shibata, T. Kiyoura, J. Kitagawa, T. Sumiyoshi and K. Tanabe, Bull. Chem. Soc. Jpn. 46 (1973) 2985;
K. Tanabe, T. Sumiyoshi, K. Shibata, T. Kiyoura and J. Kitagawa, Bull. Chem. Soc. Jpn. 47 (1974) 1064.

[19] M. Haneda, Y. Kintaichi, M. Inaba and H. Hamada, Appl. Surf. Sci., in press.

[20] K. Hadjiivanov, V. Bushev, M. Kantcheva and D. Klissurski, Langmuir 10 (1994) 464.